AIP | Journal of Applied Physics

Passivation of Zn3P2 substrates by aqueous chemical etching and air oxidation

Gregory M. Kimball, Jeffrey P. Bosco, Astrid M. Müller, Syed F. Tajdar, Bruce S. Brunschwig et al.

Citation: J. Appl. Phys. **112**, 106101 (2012); doi: 10.1063/1.4765030
View online: http://dx.doi.org/10.1063/1.4765030
View Table of Contents: http://jap.aip.org/resource/1/JAPIAU/v112/i10
Published by the American Institute of Physics.

Passivation of Zn_3P_2 substrates by aqueous chemical etching and air oxidation

Gregory M. Kimball, Jeffrey P. Bosco, Astrid M. Müller, Syed F. Tajdar, Bruce S. Brunschwig, Harry A. Atwater,[a] and Nathan S. Lewis[a]
Noyes Laboratory, Watson Laboratory, and Beckman Institute, California Institute of Technology, Pasadena, California 91125, USA

(Received 3 May 2012; accepted 12 October 2012; published online 21 November 2012)

Surface recombination velocities measured by time-resolved photoluminescence and compositions of Zn_3P_2 surfaces measured by x-ray photoelectron spectroscopy (XPS) have been correlated for a series of wet chemical etches of Zn_3P_2 substrates. Zn_3P_2 substrates that were etched with Br_2 in methanol exhibited surface recombination velocity values of 2.8×10^4 cm s^{-1}, whereas substrates that were further treated by aqueous HF–H_2O_2 exhibited surface recombination velocity values of 1.0×10^4 cm s^{-1}. Zn_3P_2 substrates that were etched with Br_2 in methanol and exposed to air for 1 week exhibited surface recombination velocity values of 1.8×10^3 cm s^{-1}, as well as improved ideality in metal/insulator/semiconductor devices. © *2012 American Institute of Physics*.
[http://dx.doi.org/10.1063/1.4765030]

With a direct band gap at 1.5 eV,[1] long (5–10 μm) minority-carrier diffusion lengths,[2] and controllable p-type doping (10^{13}–10^{18} cm^{-3}),[3] zinc phosphide (Zn_3P_2) is an interesting candidate for the active semiconductor absorber in solar energy-conversion devices. Due to the difficulty in preparing n-type Zn_3P_2, device fabrication with Zn_3P_2 has focused on *p-n* heterojunctions and Schottky diodes, with p-Zn_3P_2/Mg devices having exhibited solar energy-conversion efficiencies up to 6%.[4,5]

However, Zn_3P_2 *p-n* heterojunctions have only reached solar energy-conversion efficiencies of $\leq$2% and are limited by high concentrations of interface states.[6–8] Zn_3P_2/ZnO and Zn_3P_2/Al_2O_3 interfaces have exhibited interfacial recombination velocity values of $>10^7$ cm s^{-1} and defect distributions of $>10^{13}$ eV^{-1} cm^{-2}, respectively.[9,10] The high concentration of interface states has been related to the wet chemical preparation process, and/or to damage during physical deposition, and/or to deleterious solid-state interface reactions. Etching with Br_2 in CH_3OH has been used to prepare Zn_3P_2 surfaces for device fabrication but detailed information on the surface composition is not yet available.[11–13]

In this study, we describe the surface recombination characteristics and surface composition of chemically treated Zn_3P_2 substrates. Time-resolved photoluminescence (PL) was used to provide quantitative estimates of the surface recombination velocity (SRV) and surface defect density, whereas x-ray photoelectron spectroscopy (XPS) was used to monitor the composition of chemically treated Zn_3P_2 surfaces. Hg/Al_2O_3/Zn_3P_2 metal–insulator–semiconductor (MIS) devices were also fabricated to correlate the surface defect density distributions that were inferred from impedance measurements with the surface recombination rates that were inferred from time-resolved PL measurements.

To prepare the Zn_3P_2 substrates, red phosphorus chips and zinc shot (99.9999%, Alfa Aesar) were combined at 850 °C to form Zn_3P_2 crystals by a physical vapor transport process.[14–16] Hall-effect measurements indicated that the samples were p-type and intrinsically doped with an average hole density of $\sim 10^{15}$ cm^{-3} and a hole mobility of 18 ± 3 cm^2 V^{-1} s^{-1}. "Br-etched" samples were immersed for 30 s in 2-3% (v:v) Br_2 in CH_3OH, rinsed in CH_3OH, and dried under a stream of N_2(g). 2% Br_2 in CH_3OH yielded a bulk etch rate of $\sim$30 nm s^{-1} and resulted in surfaces with 1.3 nm RMS roughness. "HF-treated" samples were stirred rapidly in 10% HF–0.25% H_2O_2 (v:v) (aq) for 60 s, rinsed in distilled 10 MΩ cm resistivity water, and dried under a stream of N_2(g).

Steady-state PL measurements were performed using the 488 nm line of an Ar-ion laser, with the beam chopped at 10 kHz using an acousto-optic modulator. Time-resolved PL measurements were performed at 10 Hz with 70 ps, 355 nm, 1 μJ pulses that were produced by tripling the frequency of a regeneratively amplified, mode-locked, Nd:YAG laser. The high intensity of the laser pulses used for time-resolved PL was sufficient to reach the flat-band condition, by producing peak excess carrier densities of $\sim 10^{18}$ cm^{-3}. The time-resolved PL data were analyzed by numerically solving the continuity equations under the assumption of high-level injection,[16] assuming a nonradiative lifetime of 23 ± 2 ns and an ambipolar diffusion coefficient of 1 cm^2 s^{-1}.[17] The only adjustable parameter was the SRV, which was varied from 10^3 to 10^7 cm s^{-1}.[18,19]

The chemical composition of the Zn_3P_2 surfaces was monitored by XPS using a Kratos surface science instrument with monochromatic 1486.7 eV x-rays and a detection linewidth of 0.35 eV. The Zn $2p^{3/2}$ region was fit using a 9:1 Gaussian–Lorentzian function. The P 2p region was fit using a pure Lorentzian function, with the doublet area ratio constrained to 2:1 and the doublet separation constrained to 0.83 eV. The coverages of chemical overlayers were

[a]Authors to whom correspondence should be addressed: Electronic addresses: haa@caltech.edu and nslewis@caltech.edu.

calculated by the method of Seah,[20] with photoelectron escape depths that were estimated assuming monolayer thicknesses of 0.27 nm for Zn_3P_2, 0.28 nm for elemental phosphorus, and 0.23 nm for $Zn_x(PO_3)_y$.

Impedance measurements on $Hg/Al_2O_3/Zn_3P_2$ devices were performed using Hg-drop electrodes and ~60 nm insulating layers of Al_2O_3 that were deposited by electron-beam evaporation. The devices were swept from accumulation to depletion at 80 mV s^{-1} and the differential capacitance was monitored at 10 kHz with a 10 mV AC potential. The distribution of the surface state density was estimated by use of high-frequency capacitance methods,[19,21] taking $\varepsilon_{Al_2O_3} = 4.5$, $\varepsilon_{Zn_3P_2} = 11$, and a Zn_3P_2 dopant density of 10^{15} cm^{-3}.[22]

Figure 1 shows time-resolved PL decay traces and steady-state PL spectra for chemically treated Zn_3P_2 substrates. Under high-level injection, the PL decay dynamics immediately after the laser pulse were dominated by the effects of surface recombination, yielding quantitative estimates of the surface recombination velocity (Table I). Freshly polished samples did not exhibit detectable PL (black line, inset Fig. 1). However, etching with 2% Br_2 in CH_3OH yielded readily observable PL, and SRV values of $(2.8 \pm 0.1) \times 10^4$ cm s^{-1}. Br-etched samples that were further treated with 10% HF–0.25% H_2O_2 (aq) for 60 s showed an increase in steady-state PL intensity by a factor of 2.3 ± 0.2 and had SRV values of $(1.0 \pm 0.1) \times 10^4$ cm s^{-1}. Br-etched Zn_3P_2 samples that were exposed to air for 1 week showed even longer PL decays than samples that were tested immediately after chemical treatment, with SRV values of $(1.8 \pm 0.1) \times 10^3$ cm s^{-1}. Assuming similar cross sections for carrier capture, the formation of native oxides on Br-etched Zn_3P_2 samples thus passivated >90% of the electrically active surface recombination sites.

Figure 2 shows the high-resolution XPS data of the Zn $2p^{3/2}$ and P 2p regions of chemically treated Zn_3P_2 substrates. After etching with 2% Br_2 in CH_3OH for 30 s, the

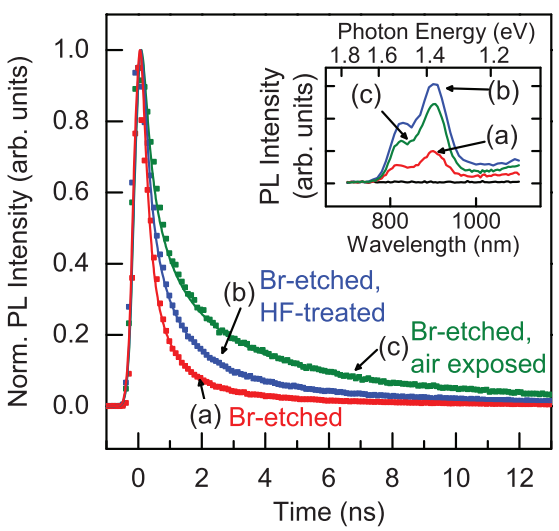

FIG. 1. Time-resolved PL decay data collected under Ar(g) at 295 K for Zn_3P_2 substrates that were (a) etched in 2% Br_2 in CH_3OH for 30 s, (b) etched in 2% Br_2 in CH_3OH for 30 s and then treated with 10% HF–0.25% H_2O_2 (aq) for 60 s, and (c) etched in 2% Br_2 in CH_3OH for 30 s and then exposed to air for 1 week. The inset shows the steady-state PL spectra that were collected in ambient conditions for Zn_3P_2 substrates with surface treatments (a), (b), and (c).

TABLE I. Photoluminescence-based characterization of chemically treated Zn_3P_2, where relative PL intensity was recorded at 890 nm, and time-resolved PL decays were used to determine surface recombination velocity (S). The surface trap density (N_t) was derived using the relationship, $S = N_t \sigma v_{th}$, assuming a carrier capture cross section $\sigma = 10^{-16}$ cm^2 and a thermal velocity $v_{th} = 10^7$ cm s^{-1}.

Sample	Relative PL signal (arb. units)	S (cm s^{-1})	N_t (cm^{-2})
Polished	<0.02	n/a	n/a
(i)	1.0 ± 0.2	$(2.8 \pm 0.1) \times 10^4$	3×10^{13}
(ii)	2.3 ± 0.2	$(1.0 \pm 0.1) \times 10^4$	1×10^{13}
(i), 1 week air	1.7 ± 0.2	$(1.8 \pm 0.1) \times 10^3$	2×10^{12}

(i) = 2% (v:v) Br_2 in CH_3OH for 30 s.
(ii) = (i) followed by 10% HF–0.25% H_2O_2 (aq) for 60 s.

substrates exhibited bulk stoichiometric Zn and P species, 0.4 ± 0.2 monolayers of oxidized zinc, 0.3 ± 0.1 monolayers of oxidized phosphorus, and 4.1 ± 0.5 monolayers of elemental phosphorus (P^0) (Fig. 2(a)). Treatment of the Br-etched substrates with 10% HF–0.25% H_2O_2 (aq) for 60 s decreased the P^0 surface coverage to 1.4 ± 0.2 monolayers without introducing additional surface oxidation of Zn or P species (Fig. 2(b)). Substrates that had been etched with 2% Br_2 in CH_3OH for 30 s and then exposed to air for 1 week (Fig. 2(c)) showed oxidized phosphorus and oxidized zinc signals that were consistent with the presence of 4 ± 2 monolayers of $Zn_x(PO_3)_y$ species. Table II shows the binding energies and Gaussian peak widths observed for the surface zinc and phosphorus species of the series of Zn_3P_2 surfaces.

Figure 3 compares the normalized capacitance data collected from $Hg/Al_2O_3/Zn_3P_2$ devices to the expected ideal performance in the absence of surface trap states. Ideal MIS devices with p-type semiconductors show decreasing capacitance with increasing positive gate bias as the semiconductor is swept into depletion. However, freshly Br-etched Zn_3P_2 substrates showed only a small modulation of capacitance with gate bias, consistent with a high density of surface defects ($>10^{13}$ eV^{-1} cm^{-2}). The capacitance data from Br-etched Zn_3P_2 substrates that had been exposed to air for 1 week instead showed a significant depletion of the semiconductor at positive gate bias, and allowed for an estimate of the surface trap density distribution, D_t, of $\sim 10^{12}$ eV^{-1} cm^{-2} (Figure 3 inset). The surface trap density distributions derived from capacitance measurements of MIS devices were consistent with the surface trap density values that were derived from time-resolved PL measurements.

The estimated surface trap density values in Table II support the hypothesis that the electronic quality of the surface prepared by etching with 2% Br_2 in CH_3OH limits the performance of the resulting Zn_3P_2 devices, rather than damage during physical deposition or deleterious solid-state interface reactions. The presence of residual P^0 correlated with poor electronic quality in that the coverage of P^0 and the surface recombination rates both decreased after treatment of Br-etched Zn_3P_2 substrates with 10% HF–0.25% H_2O_2 (aq). A low residual P^0 coverage on Zn_3P_2 thus appeared to reduce the surface trap density and offers a promising approach to unpin the Fermi level in *p-n*

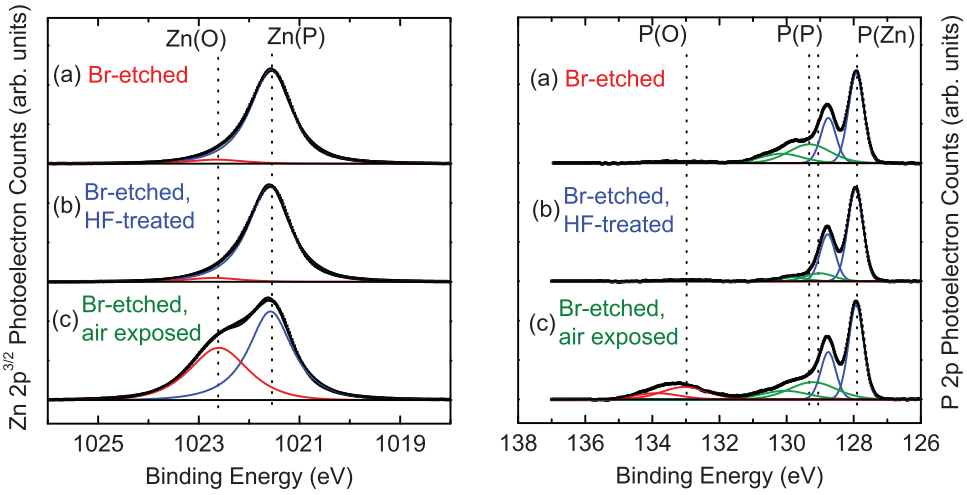

FIG. 2. X-ray photoelectron spectra of the Zn $2p_{3/2}$ and P $2p$ regions for Zn_3P_2 substrates that were (a) etched in 2% Br_2 in CH_3OH for 30 s, (b) etched in 2% Br_2 in CH_3OH for 30 s and then treated with 10% HF–0.25% H_2O_2 (aq) for 60 s, and (c) etched in 2% Br_2 in CH_3OH for 30 s and then exposed to air for 1 week.

TABLE II. XPS core binding energies for Zn $2p_{3/2}$ and P $2p_{3/2}$ signals, including bulk Zn_3P_2, residual elemental phosphorus, and native oxide.

Core level	Species	Binding energy (eV)	Gaussian width (eV)
Zn $2p_{3/2}$	Zn_3P_2	1021.6 ± 0.1	0.96 ± 0.02
Zn $2p_{3/2}$	ZnO_x	1022.6 ± 0.1	1.4 ± 0.1
P $2p_{3/2}$	Zn_3P_2	127.9 ± 0.1	0.54 ± 0.02
P $2p_{3/2}$	P^0	129.1 ± 0.2	1.3 ± 0.2
P $2p_{3/2}$	PO_x	133.0 ± 0.3	1.5 ± 0.1

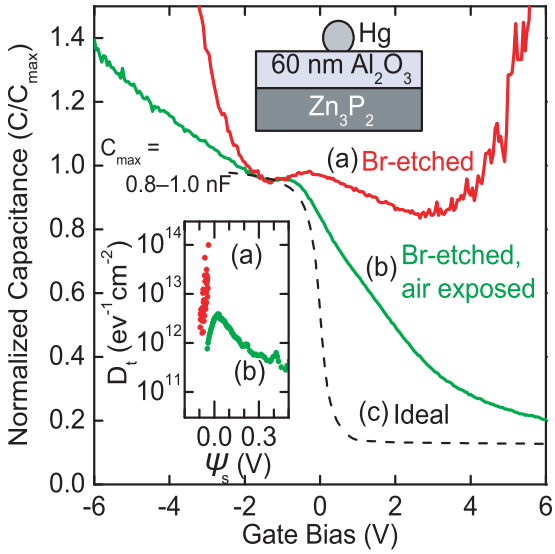

FIG. 3. High-frequency (10 kHz) capacitance as a function of gate bias for $Hg/Al_2O_3/Zn_3P_2$ devices where the substrate was (a) etched in 2% Br_2 in CH_3OH for 30 s, or (b) etched in 2% Br_2 in CH_3OH for 30 s then exposed to air for 1 week. Trace (c) shows the expected capacitance for ideal $Hg/Al_2O_3/Zn_3P_2$ devices in the absence of surface trap states. The inset shows the estimated surface trap density distribution D_t as a function of surface potential Ψ_s for $Hg/Al_2O_3/Zn_3P_2$ devices.

heterojunction devices. The surface recombination velocity values of $<2 \times 10^3$ cm s^{-1}, and the improved MIS performance of oxidized Zn_3P_2 surfaces, highlight the potential of the method for surface passivation and device integration. The data suggest that the native oxides of Zn_3P_2 are similar to those of InP, which have been incorporated in high efficiency MIS solar cells,[23] motivating further effort to apply physical and/or chemical oxidation techniques to Zn_3P_2 prior to device integration.

This work was supported by the Department of Energy under Grant Nos. DE-FG02-03ER15483 and DE-FG36-08GO18006, by the Beckman Institute Laser Resource Center, and by the Dow Chemical Company. GMK acknowledges support by an NDSEG graduate fellowship and Jeffery W. Lefler is acknowledged for fabrication of a custom time-resolved photoluminescence chamber.

[1]G. M. Kimball, A. M. Muller, N. S. Lewis, and H. A. Atwater, Appl. Phys. Lett. **95**, 112103 (2009).
[2]N. C. Wyeth and A. Catalano, J. Appl. Phys. **50**, 1403 (1979).
[3]G. M. Kimball, N. S. Lewis, and H. A. Atwater, in *Proceedings of IEEE 35th Photovoltaic Specialist Conference, Honolulu, HI, 20–25 June 2010*, (IEEE, New York, 2010), p. 1039.
[4]M. Bhushan and A. Catalano, Appl. Phys. Lett. **38**, 39 (1981).
[5]N. C. Wyeth and A. Catalano, J. Appl. Phys. **51**, 2286 (1980).
[6]M. Ginting and J. D. Leslie, Can. J. Phys. **67**, 448 (1989).
[7]T. Suda, M. Suzuki, and S. Kurita, Jpn. J. Appl. Phys., Part 2 **22**, L656 (1983).
[8]P. S. Nayar and A. Catalano, Appl. Phys. Lett. **39**, 105 (1981).
[9]M. Casey, J. Appl. Phys. **61**, 2941 (1987).
[10]P. S. Nayar, J. Appl. Phys. **53**, 1069 (1982).
[11]A. J. Nelson, L. L. Kazmerski, M. Engelhardt, and H. Hochst, J. Appl. Phys. **67**, 1393 (1990).
[12]Y. Kato, Appl. Phys. Lett. **52**, 2133 (1988).
[13]U. Elrod, M. C. Luxsteiner, M. Obergfell, E. Bucher, and L. Schlapbach, Appl. Phys. B: Photophys. Laser Chem. **43**, 197 (1987).
[14]A. Catalano, J. Cryst. Growth **49**, 681 (1980).
[15]G. M. Kimball, N. S. Lewis, and H. A. Atwater, in *Proceedings of IEEE 33rd Photovoltaic Specialist Conference, San Diego, CA, 11–16 May 2008*, (IEEE, New York, 2008), p. 150.
[16]See supplementary material at http://dx.doi.org/10.1063/1.4765030 for substrate orientation maps collected by electron backscattered diffraction; MATLAB code used for numerical simulation of time-resolved photoluminescence data.
[17]S. W. Feldberg, M. Evenor, D. Huppert, and S. Gottesfeld, J. Electroanal. Chem. **185**, 209 (1985).
[18]M. Bhushan, J. Appl. Phys. **53**, 514 (1982).
[19]S. M. Sze and K. K. Ng, *Physics of Semiconductor Devices*, 3rd ed. (Wiley-Interscience, 2006).
[20]M. P. Seah, *Practical Surface Analysis*, 2nd ed. (John Wiley & Sons, Chichester, 1990).
[21]L. M. Terman, Solid-State Electron. **5**, 285 (1962).
[22]J. Misiewicz, J. M. Wrobel, and B. P. Clayman, Solid State Commun. **66**, 747 (1988).
[23]K. Kamimura, T. Suzuki, and A. Kunioka, Appl. Phys. Lett. **38**, 259 (1981).